ADVANCED FUNCTIONAL MATERIALS
www.afm-journal.de

Self-Supporting Graphene Hydrogel Film as an Experimental Platform to Evaluate the Potential of Graphene for Bone Regeneration

Jiayu Lu, Yu-Shi He, Chi Cheng, Yi Wang, Ling Qiu, Dan Li, and Derong Zou**

Graphene, a two dimensional carbonaceous material possessing a range of extraordinary properties, is considered promising for biomedical applications. Here, a simple form of graphene-based bulk material–self-supporting graphene hydrogel (SGH) film is used as a suitable platform to study the intrinsic properties of graphene both in vitro and in vivo. The free-standing film show good cell adhesion, spreading, and proliferation. Films are implanted into subcutaneous sites of rats, and produce minimal fibrous capsule formation, and mild host tissue response in vivo. New blood vessel formation is also seen. The films swell and cracked in vivo, indicating the beginning of degradation. Of particular interest is that the film alone is found to be able to stimulate osteogenic differentiation of stem cells, without additional inducer, both in vitro and in vivo. Thus, this SGH film appears to be highly biocompatible and osteoinductive, demonstrating graphene's potential for bone regenerative medicine.

1. Introduction

Recently, a growing amount of work is seen to explore the potential of graphene, the two-dimensional carbon allotrope, for possible applications in biomedical and regenerative engineering.[1–4] To date, the application prototypes proposed are voluminous covering topics including biosensing,[5–8] imaging,[9] drug delivery,[10,11] chemo-photothermal therapy,[12,13] antibacterial properties,[14,15] and tissue engineering[16] that exploiting one or simultaneously a few aspects of the many extraordinary electrical, optical, thermal, and mechanical properties of graphene.[17–29] Most of previous investigations have been devoted to understanding the unilateral response of an organism to the enabling function chosen of graphene. Nevertheless, to evaluate the potential of graphene as an alternative biomaterial comes down to the study of the interactions between the material and a living body. The effect an in vivo surrounding to graphene, such as the possible bio-degradation of graphene, which is equally of importance in evaluating a biomaterial, remains largely unclear. In this regard, efforts are to expect in elucidating this bilateral dependence between graphene and a living organism particularly in vivo.

To properly investigate and objectively present the effect of an organism to graphene can be experimentally challenging. Most of the studies/applications reported thus far were performed/demonstrated using graphene suspensions,[24] which can be easily scattered and drained away by body fluids, making it difficult to locate and monitor their behavior. Under an optical microscope, which is now still the main observation tool for studying cell spread and morphology, graphene single layers are invisible; the black spots usually observed under an optical microscope are in fact graphene aggregates, whose behavior can be different from that of individually separated graphene sheets. On the other hand, substrate-supported graphene sheets, another form widely adopted for cell biology study,[16,27] may also not be suitable for an objective evaluation, as researches have shown that the properties of these supported sheets can be severely influenced by the nature of underlying substrates.[30] Therefore, a proper form of graphene capable of fulfilling objective evaluation of its biomedical properties is sought after.

In response to this call, we have designed a self-supporting graphene hydrogel (SGH) film by rationally manipulating the colloidal interactions among solvated graphene sheets.[31,32] The film is purely composed of graphene and has a simple multilayered structure. Due to intrinsic corrugation of graphene and solvation repulsion between neighboring graphene sheets, the graphene sheets inside SGHs remain largely separated; thus the in vivo behavior of SGHs can be treated as that of a large amount of separated graphene sheets in a collective manner. Moreover, this graphene bulk film has a dimension comparable to that of cells, making itself easily being located under

J. Lu, Y. Wang, Prof. D. Zou
Department of Stomatology
the Sixth People's Hospital Affiliated to
Shanghai Jiao Tong University
No. 600, Yishan Road, Xuhui District,
Shanghai, 200233, P. R. China
E-mail: derongzou@gmail.com
Dr. Y.-S. He
Institute of Electrochemical and Energy Technology
Department of Chemical Engineering
Shanghai Jiao Tong University
Shanghai, 200240, P. R. China
C. Cheng, L. Qiu, Prof. D. Li
Department of Materials Engineering
Monash University
VIC 3800, Australia
E-mail: dan.li2@monash.edu

DOI: 10.1002/adfm.201203637

an optical microscope. Without any binders or crosslinkers, SGHs render exceptional mechanical flexibility and adaptability. As it is chemical/biochemical stable and can remain in one location for a reasonable long period of time (three months or even longer), the graphene film is particularly suitable for direct monitoring in vivo.

Previous research has shown that graphene helps accelerate specific differentiation of stem cells into bone cells.[16,33] As a proof-of-concept, in this study, we used the SGH film as an experimental platform to evaluate the potential of graphene particularly for bone regeneration. By implanting the SGH film into subcutaneous sites of rats, we investigated the host tissue response and evaluated the biocompatibility in vivo. Interestingly, we found that SGH film not only rendered highly biocompatible, but intrinsically osteoinductive even without the aid of any external inducer. More importantly, the initial stage of bio-degradation of SGH films was observed, which sheds new light on the complicated yet crucial interaction between graphene and an organism, providing valuable information particularly for future efforts on exploiting graphene for bone regeneration application.

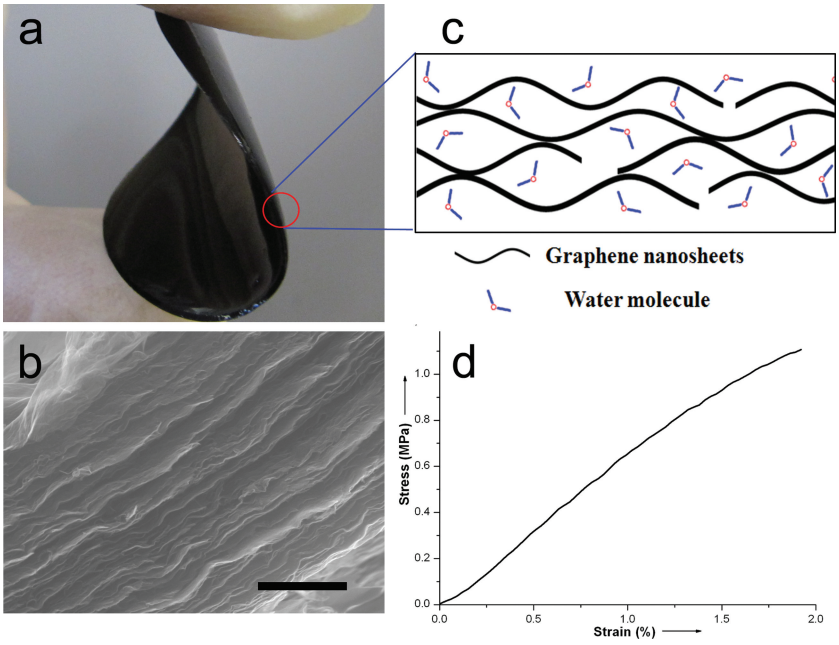

Figure 1. Characterization of the SGH film. a) Photograph of the as-formed flexible SGH film. b) SEM image of the cross-section of a freeze-dried SGH film. Scale bars: 1 µm. c) Schematic of the cross-section of SGH film, indicating the water molecules separate the nanosheets. d) Typical stress–strain curve of an SGH film.

2. Results and Discussion

2.1. Preparation and Characterization of SGH Film

To prepare the SGH films, a certain amount of chemically converted graphene (CCG) dispersion was filtered through a mixed cellulose ester filter membrane via direct-flow vacuum filtration. When the filtration just completed (no CCG dispersion left on the filter), the as-formed wet SGH film was directly peeled off from the filter membrane (**Figure 1**a) and cut into sizes required for various tests without further drying (Supporting Information Figure S1). Scanning electron microscopy (SEM) analysis of a freeze-dried sample revealed a uniform multilayered and wrinkled structure (Figure 1b). The as-formed SGH film gives no distinct X-ray diffraction (XRD) peak at around 23° as is commonly found in the dried graphene paper (Supporting Information Figure S2), and the average interlayer spacing in SGH films was estimated to be around 10 nm.[34] Further dynamic electrosorption analysis shows a significant increase in the electrosorption capacity of SGH films compared to their dried counterparts.[35] These results prove that the graphene sheets in the SGH film remain largely separated, allowing the surface area of each individual graphene sheets to maximally interact with their surroundings (Figure 1c).[34] Despite being highly porous and containing ≈90% water, the SGH film renders excellent mechanical flexibility, and is mechanically strong with an average tensile modulus of (69 ± 5) MPa (Figure 1d), comparable to that of typical rubbers.[32] This remarkable mechanical strength is a valuable feature of a suitable biomaterial particularly required for bone regeneration. SEM images of the cross-section (Figure 1b) and surface (**Figure 2**a) of the freeze-dried SGH films, as well as the retention of the highly open pore structure (≈3–13 nm) of SGH film[36] revealed a wrinkled and rippled nanoscale surface morphology. With all these structural and physical properties combined, SGH films can thus be regarded as a good candidate

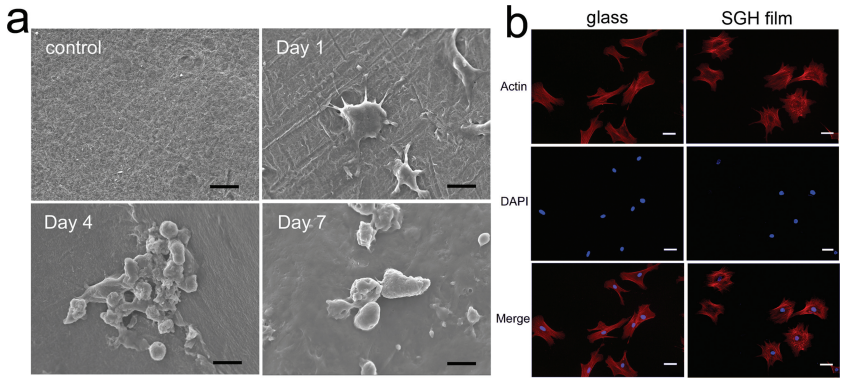

Figure 2. Cell adhesion and morphology on SGH film. a) SEM images of SGH film as control and adhesion of cells onto SGH film surfaces at 1, 4, and 7 days after seeding. Scale bars: 10 µm. b) Actin filament network (red), DAPI-stained nucleus (blue) and merged images of cell morphologies on SGH film and glass, 24 h after seeding. Scale bars: 50 µm.

and an experiment platform to evaluate the potential of graphene for bone regeneration.

2.2. Cell Adhesion, Morphology, Proliferation, and Cytotoxicity on SGH Film

To start evaluating the biocompatibility and osteoinductivity of the SGH film, we chose rat bone marrow stromal stem cells (rBMSCs), which are known to have osteogenic differentiation potency after osteogenic induction (Supporting Information Figure S3), to examine their adhesion and growth on this unique macroscopic graphene assembly. As shown in Figure 2a, the rBMSCs attached tightly on the surface of the SGH film and appeared flat in shape at day 1 after seeding, and then the cells spread well at day 4 and reached confluence at day 7. The cell morphology was observed 24 h after seeding on both SGH film and control glass. Interestingly, in comparison to the typical fibroblastic morphology on glass, the rBMSCs on the SGH films appeared much flatter, better spread, and showed osteoblastic morphology (Figure 2b). More cellular microextensions and larger extending areas were observed on the SGH film surface, and actin filaments had regular directions. These indicate that rBMSCs have better adaptation, proliferation and differentiation on SGH surfaces,[37] which are likely due to the high specific surface area, surface morphology, and reasonable number of functional groups on the SGH film.[31,32]

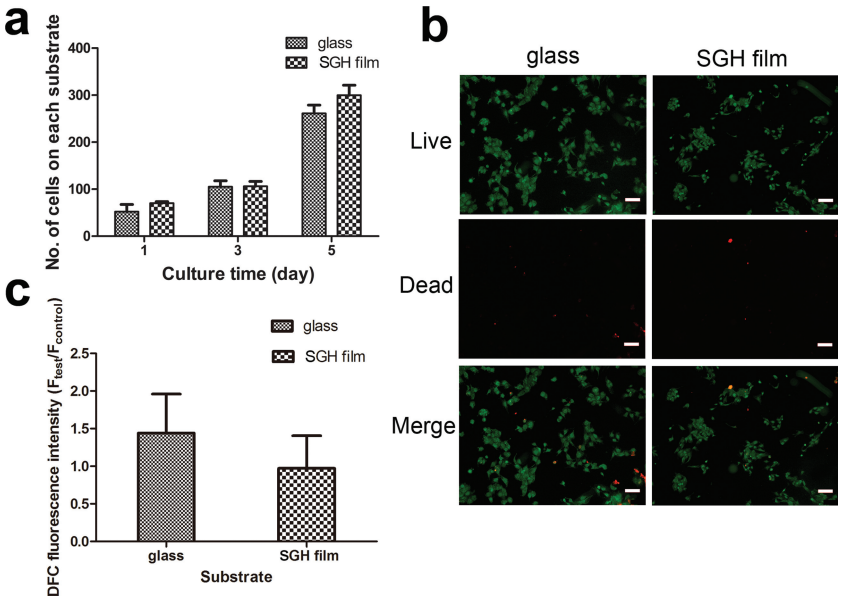

Figure 3. Cell proliferation and cytotoxicity on SGH films. a) The proliferation rates, which were calculated by counting the number of DNA-intercalating fluorochrome DAPI per unit area on glass and on SGH films from 1 to 5 days, show no significant differences between the two groups. b) Live/dead double staining, 24 h after cell seeding on glass and on SGH film. Live cells were stained florescent green, and dead cells appeared red. Note that there was no obvious difference between the cells seeded on glass and on the SGH film, indicating nontoxicity of the film. Scale bars: 100 µm. c) ROS levels of cells, 24 h after seeding, on glass and on SGH film. The ROS level of cells on SGH film was lower than that on glass, also showing the good biocompatibility of the film.

The proliferation assay was examined by comparing the cell numbers in **Figure 3**a. There was no significant difference in cell proliferative capacity between the SGH film and the glass control, with a capacity slightly higher on the SGH film (Supporting Information Figure S4).[38] This implies that the SGH film does not display cytotoxicity, which can be further supported by the results of live/dead double staining (Figure 3b) and the reactive oxygen species (ROS) generation assay (Figure 3c). The methylthiazolyldiphenyl-tetrazolium bromide (MTT) assay analysis was also used to detect cell proliferation on graphene.[39,40] As shown in Supporting Information Figure S5, the increasing proliferation rate of cells seeded on the SGH film was lower than that of the control group, which was also consistent with Lim et al.'s work.[39] The result could be ascribed to the high adsorption of MTT product purple formazan by graphene, indicating the MTT assay was not suitable for detecting cell proliferation on the SGH film.

2.3. Implantation of SGH Film

In vivo study was carried out by implanting the SGH films into subcutaneous dorsum sites of rats. No noticeable toxic side effects for the implanted SGH films in rats were observed within 12 weeks after implantation. All samples recovered well and body weight remained stable after surgery, and no noticeable signs of major organ damage (lung, liver, spleen, kidney, heart) were observed during the observation period (Supporting Information Figure S6). The SGH films still maintained their structures over the study period in the gross specimens. The ability of remaining its original location for a period of time could be beneficial to offer initial structural support for a bone defect.

When implanted into living tissue, all materials initiate a host response that reflects the first steps of tissue repair. It is noted that the innate immune system plays an major role in determining the biocompatibility of biomaterials, and typically, in vivo implantation of biomaterials leads to tissue-specific responses by macrophages or foreign body giant cells.[41] Since the practical use of clinical biomaterials may be affected by the induction of a post-implantation host tissue response, the development of suitable biomaterials must include the minimization of post-implantation host tissue responses. Histological images obtained using hematoxylin and eosin (HE) staining showed that the subcutaneously implanted SGH films were all encapsulated at week 2, when slight inflammation and expansion of blood vessels were observed (**Figure 4**). The early inflammation could also be due to injury from the surgery.[42] Host tissue response, in the form of macrophages, was observed at week 4. At the same time, fibroblasts and thin fibrous connective tissue were found surrounding the films. The response appeared to be localized and had eased by week 8. At week 12, a thin layer of fibrous capsule and new blood vessels could be seen around the SGH films (Figure 4 and Supporting Information

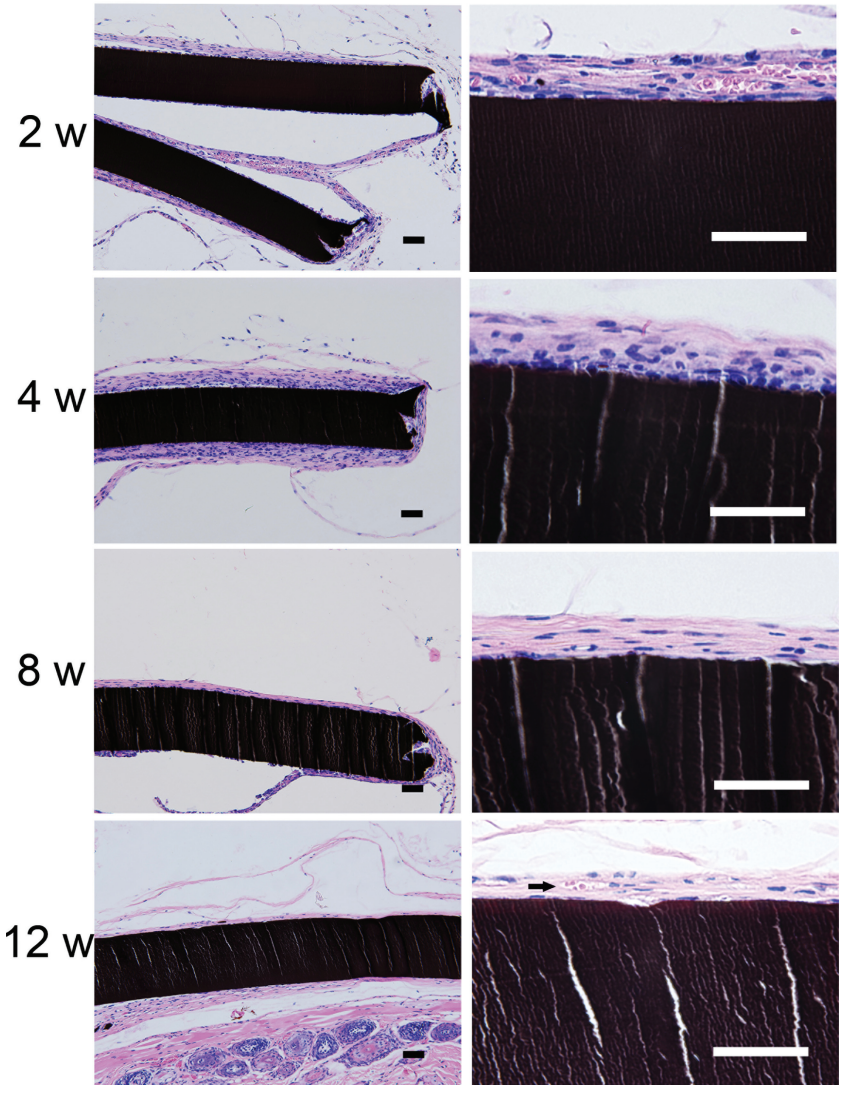

Figure 4. Histological images with HE staining of the SGH films from 2 to 12 weeks after implantation. The films were encapsulated at week 2 with slight inflammation and expansion of blood vessels. Host tissue response was observed at week 4 with macrophages as well as fibroblasts and thin fibrous connective tissue surrounding the implant. The tissue response had subsided by week 8. At week 12, there was a thin layer of fibrous capsule around and a new blood vessel (Arrow) could be seen near the film. Scale bars: 50 μm.

Figure S7). The macroscopically usable SGH films implanted into the subcutaneous space of rats rendered minimal fibrous capsule formation, mild host tissue response and formation of new blood vessels, indicating a foreign body–type reaction. No severe inflammatory response such as necrosis, degeneration, or neutrophil infiltration was observed around the films throughout the experimental period, indicating the film was a safe biomaterial for the living body.

Out of expectation, we have observed initial stage of biodegradation of the implanted SGH films. Cracked graphene chips were seen on both ends of the films with the appearance of multinucleated foreign body giant cells (FBGCs) and abundant blood vessels (**Figure 5**a). Chips were also found encased by the FBGCs (Supporting Information Figure S8), indicating the active absorption of graphene-based bulk materials by cell-mediated phagocytosis.[43] The abundance of blood vessels indicated that the chips of SGH films could also be cleared from systemic blood circulation.[44]

In Figure 5b, the thicknesses of the implanted films were shown and excitingly, the films were found to be thicker as the observation time went on. As has been suggested that hydrogel materials containing hydrophilic oxygen-containing groups become swelled in the physiological environment,[45] we reason that the absorption of molecules from the body fluid might reduce the π–π interaction between CCG sheets in the hydrogel, resulting in an increase of interlayer spacing. The swelling and cracking of the film, as well as cell-mediated phagocytosis, strongly suggest initiation of degradation of this graphene bulk film in living body. Such a feature could be highly advantageous because a degradable graphene film could first serve as a guide for the ingrowth of the newly formed bone and then degrade, avoiding a second surgery to extract the implant. Nevertheless, longer-term study on the toxicology and degradation behavior of the graphene films is required to explore their application in this regard.

2.4. Osteogenic Differentiation of rBMSCs on SGH Film

A biomaterial for bone regeneration will act as a matrix for cell proliferation, osteogenic differentiation, extracellular matrix deposition and new bone tissue formation.[46] The ability of SGH films to enhance osteogenic differentiation of rBMSCs was another focus of this study. Typically, chemically induced osteogenic differentiation on culture dishes takes 21 days to complete.[47] Alkaline phosphatase (ALP), which regulates organic or inorganic phosphate metabolism by hydrolysis of phosphate esters, and acts as a plasma membrane transporter for inorganic phosphates, can be used as an early marker for osteoblastic cell differentiation.[48] In this study, the ALP activity of cells cultured on the SGH films in osteogenic medium increased noticeably at day 4 after incubation (**Figure 6**a). A statistically higher level was observed for the cells on the SGH films compared to those on the control either in osteogenic or growth medium at day 7 after seeding. The enhancement of osteogenic differentiation was also confirmed by immunofluorescence staining of osteocalcin (OCN), a marker of osteogenic differentiation related to matrix deposition and mineralization.[49] Figure 6b shows the immunofluorescence expression for OCN protein; OCN increased remarkably at day 4 after seeding and reached a maximum at day 7 on SGH films either

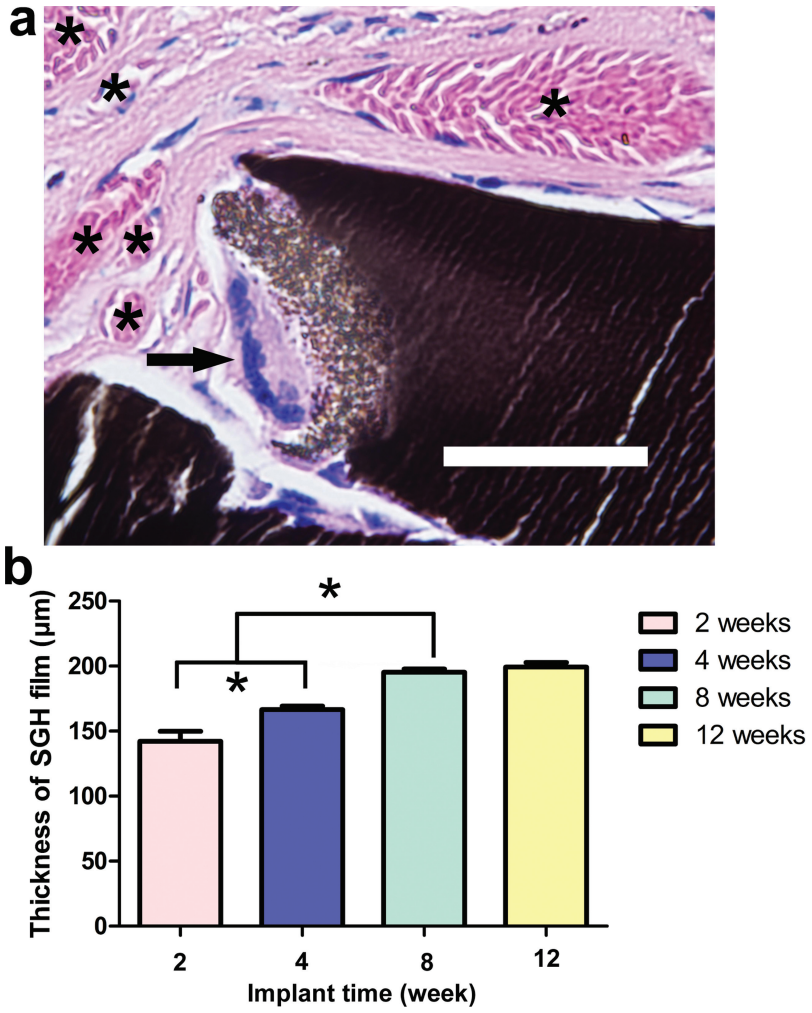

Figure 5. Changes of the SGH films in the living body. a) HE staining of SGH film, 12 weeks after implantation. Cracked graphene chips were observed on the edge of the films with the appearance of foreign body giant cells (arrow) and an abundance of blood vessels (B). Scale bar: 50 μm. b) The thickness of the SGH films from 2 to 12 weeks after implantation. Note that the films became thicker as the observation time increased. (*$p < 0.01$).

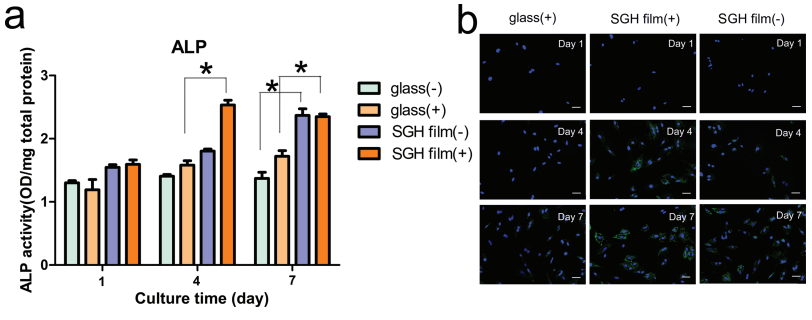

Figure 6. Osteogenic differentiation of rBMSCs on SGH films. a) ALP activity of cells growing on glass and on the SGH film at 1, 4, and 7 days after seeding. (–): growth medium. (+): osteogenic medium. Note that the ALP activity of the cells seeded on the SGH film in osteogenic medium increased clearly at 4 and 7 days after incubation, while that in growth medium increased clearly at 7 days after incubation (*$p < 0.01$). b) Immunofluorescence staining for OCN of cells growing on glass and on the SGH film at 1, 4, and 7 days after seeding. OCN of cells on the SGH film became visible at 4 days and intense at 7 days after seeding in both osteogenic and growth media. Scale bars: 50 μm.

in osteogenic or growth medium. The cells on the control glass showed weaker fluorescence, as also seen in the study by Nayak et al.[33] These results showed that the SGH film alone was adequate to induce osteogenic differentiation of rBMSCs in growth medium, while promotion of osteogenic differentiation of the stem cells on the SGH film occurred much earlier and more strongly in osteogenic medium supplemented with L-ascorbic acid, glycerophosphate and dexamethasone. The positive Alizarin Red S staining strongly supports our findings that graphene could effectively enhance the osteogenic differentiation and calcium deposits of stem cells (Supporting Information Figure S9). This demonstrates that the SGH films were osteoinductive and produced enhanced osteogenic differentiation in the early stages.

The osteoinductive ability of the SGH film was also studied in vivo. In **Figure 7**, red fluorescence of (please approve changes) OCN was observed on the right surface of the film, where rBMSCs seeded on the films were induced to become bone-forming cells. On the left side, without rBMSCs, no obvious fluorescence was seen. We also confirmed that the rBMSCs grew and remained on the surface of the material for 4 weeks in vivo. The subcutaneous site was a nonosseous environment,[50] where the only factor which could induce the cells to become bone-forming osteoblasts was the SGH film.

The excellent osteoinductive ability of the SGH film could be largely attributed to its surface morphology and mechanical properties. The surface morphology is the decisive factor for osteogenic differentiation.[51,52] Rough and disordered surfaces have been reported to induce bone cell differentiation.[53] Graphene with its ripples and wrinkles could strongly adsorb proteins and enhance cell growth and differentiation.[33] The corrugated and porous surface of the SGH film also could provide anchor points for the cytoskeletons and impact on cytoskeletal tension, which changes the cell morphology (Figure 2b). It is reported that the cell morphology regulates the switch in lineage commitment by modulating endogenous RhoA, an important small G-protein involved in cell signaling and cytoskeletal organization.[51] Cells with flattened and well-spread shapes will undergo osteogenesis,[51] as will the rBMSCs on the SGH film.

Another important aspect that helps explain why the SGH shows osteogenetic property is the exceptional mechanical property of SGH films. The SGH films have an average tensile modulus of (69 ± 5) MPa (Figure 1d), which is much higher than those of conventional polymer hydrogels with similar water content (usually reported in the range of 0.01 to 10 kPa).[32] It has

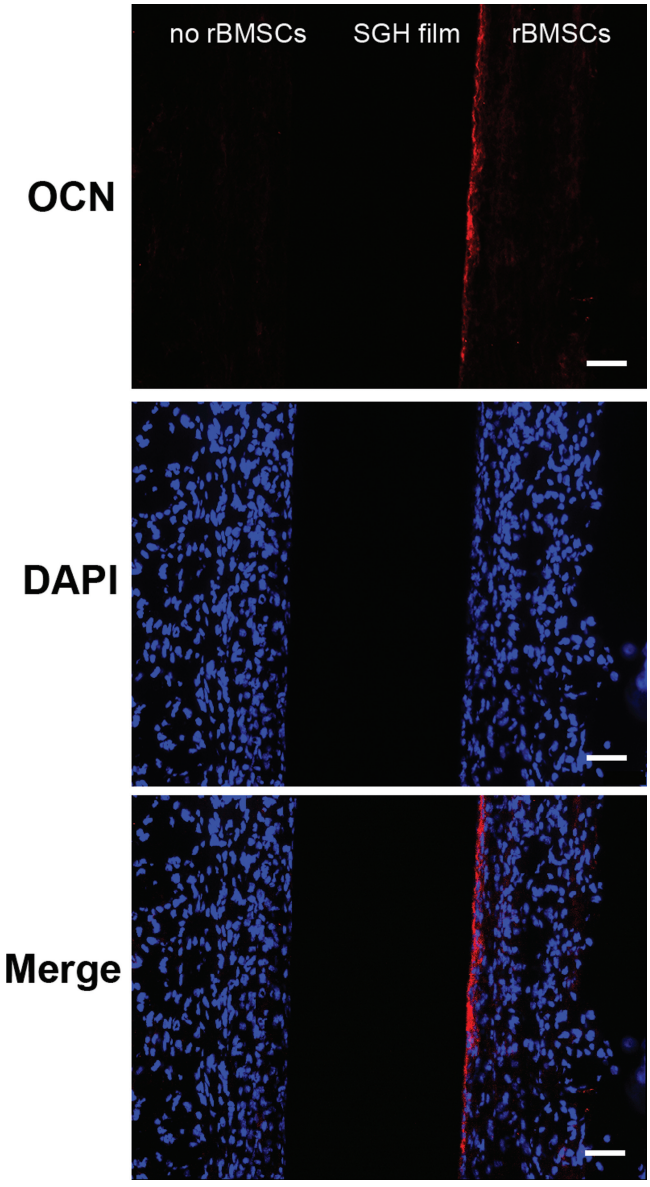

Figure 7. Immunofluorescence staining for OCN of the SGH film at 4 weeks after implantation. Red fluorescence was seen on the right surface of the film (with rBMSCs), while on the left side (without rBMSCs), no obvious fluorescence was seen. It was considered that the rBMSCs were induced to become bone-forming cells by the SGH film. Scale bars: 50 μm.

been reported by Engler et al. that stiff substrates could promote bone differentiation.[54] Therefore, it is reasoned that the exceptional mechanical property of SGH films could play a role in stimulating stem cell differentiation.[16,33] Although other possible mechanisms of osteoinductivity of graphene should be further explored, our research shows that graphene has great potential to make a bona fide alternative to autograft and xenograft therapies, avoiding the negative side effects of bone harvesting and potential induction of transmissible diseases. Further research is needed to evaluate if such graphene films could compete with traditional osteoinductivity biomaterial–demineralized bone matrix.[55]

3. Conclusions

We used a macroscopic free-standing chemically converted graphene hydrogel film as an experimental platform to examine the biocompatibility and osteoinductivity of graphene. The SGH film enhanced cell adhesion, spreading and proliferation. Moreover, when implanted into subcutaneous sites of rats, the SGH film induced minimal fibrous capsule formation, a mild host tissue response and yielded no obvious signs of toxic side effects, indicating in vivo biocompatibility and nontoxicity of the film. Cracking began from both ends of the material and the detached particles then migrated by cell-mediated phagocytosis and incorporation into the blood circulation system. Interestingly, the films became thicker with an increase of implantation time, suggesting that the hydrogel swelled in the physiological environment. The swelling and cracking of the films proved that degradation began after implantation. In particular, we found that the graphene hydrogel film could induce the regeneration of bone without the need for any additional inducer. The present study has deepened our understandings of the biological behavior of graphene both in vitro and in vivo. A combination of good biocompatibility, osteoinductivity, appropriate mechanical strength and potential degradability of the film makes it potentially attractive for biomedical applications, especially as a "smart" biomaterial for bone regeneration. For example, the SGH film in this study may serve as a kind of special biological membrane with osteoinductivity in the guided bone regeneration (GBR) technique of oral biomedicine.

4. Experimental Section

Preparation of Self-Supporting Graphene Hydrogel (SGH) Films: Chemically converted graphene (CCG) was prepared by chemical reduction of a graphene oxide solution that was obtained by chemical oxidation and exfoliation of natural graphite. The synthetic procedure of CCG dispersion has been reported in our previous publication.[56] To prepare the SGH film, a certain amount of CCG dispersion (0.37 mg/mL) was filtered through a mixed cellulose ester filter membrane (0.05 μm pore size; Millipore Co., USA) by vacuum suction.[32] Once the filtration was completed, the relatively thick films were carefully peeled off from the filter membrane using tweezers and then used for various measurements. All SGH films were stored in water prior to use. The films were cut into required sizes using scissors for various tests.

Structure and Characterization of SGH Film: Scanning electron microscopy (SEM, JSM 7001F; JEOL, Japan) images were used to examine the morphology of the freeze-dried films (Alpha 1-2; Christ, Germany). X-ray diffraction (XRD) patterns were recorded on a X-ray diffractometer (1130; Philips, Netherlands) with copper radiation (40 kV, 25 mA, Cu Kα, λ = 1.5418 Å) at room temperature. The data were collected from 5° to 50° with the scan rate of 2° min^{-1} and steps of 0.02°. Tensile properties were measured on a dynamic mechanical thermal analyzer (DMTA, Mark IV; Rheometrics, USA). The samples were cut by scissors into 5 mm × 15 mm rectangular strips and then gripped through a film tension clamp. A controlled strain rate mode was used to test the mechanical properties of SGH films. The strain ramp rate was 0.01% s^{-1} and the preload was 0.02 N.

Isolation, Culture and Seeding of Rat Bone Marrow Stromal Stem Cell (rBMSCs): To test the effect of SGH films on cells growth and bone induction, we used a primary rBMSC culture technique.[57] The experimental protocol was formally approved by the Animal Care and Experiment Committee of the Sixth Peoples Hospital affiliated to Shanghai Jiao Tong University, School of Medicine. Briefly, rBMSCs were obtained from the femurs of young 40- to 43-day-old, 110–120 g, male Fischer rats. The rats were sacrificed by cervical dislocation, and the femurs were excised under aseptic conditions. Then the epiphyses were cut off, and each femur was flushed out with growth medium: Dulbecco's modified Eagle's medium (DMEM; Gibco, USA) containing 10% fetal bovine serum (v/v) (FBS; Gibco, USA), 100 U/mL penicillin and 0.1 mg/mL streptomycin (Invitrogen, USA), until the bone appeared blanched (about six or eight times). The cells were suspended and cultured in 10 mm culture dishes (Coring, USA) maintained in a humidified 37 °C/5% CO_2 incubator. After 7 days of primary culture, cells were then passaged and expanded for future use.

After being rinsed in distilled water three times, all SGH films were autoclaved at 125 °C/0.14 MPa for 30 min and then incubated in culture medium for 24 h before the following cell seeding studies. The cells were resuspended in fresh culture medium, and then loaded on SGH films and glass slides respectively. A seeding density of 5×10^3 cells/film was used for studies on attachment and proliferation, while a higher density of 2×10^4 cells/film (near confluence) was used for osteogenic differentiation assays as previously described.[58]

Adhesion and Growth of Seeded rBMSCs: The rBMSCs were cultured on SGH films for 1, 4, and 7 days, then fixed in 2.5% glutaraldehyde overnight at 4 °C and freeze-dried (Alpha 1-2; Christ, Germany). Finally the samples were sputter-coated with gold and examined by SEM (JSM 7001F; JEOL, Japan) to observe the adhesion and growth of BMSCs on the films.

Morphology of Seeded rBMSCs: The morphology of seeded rBMSCs was viewed by labeling the actin cytoskeletons using Phalloidia-TRITC (Sigma, USA) as previously described. Briefly, the rBMSCs were cultured on SGH film and glass slide for 24 h, and then fixed in 4% paraformaldehyde at room temperature for 30 min. After treating with 0.1% Triton X-100 for 20 min to permeabilize the cells and blocking with 1% albumin from bovine serum (BSA, Sigma, USA) for 20 min, the actin cytoskeletons were labeled by incubating with Phalloidia-TRITC for 30 min. Lastly, the cell nuclei were contrast-labeled in blue using 2-(4-amidinophenyl)-6-indolecarbamidine dihydrochloride (DAPI, sigma, USA) and mounted using Fluoromount (Sigma, USA). The actin cytoskeletons of cells were visualized with a fluorescence microscope (DMI6000B; Leica, Germany).

Proliferation of Seeded rBMSCs: The methylthiazolyldiphenyl-tetrazolium bromide (MTT) assay was used to determine the proliferation rate of rBMSCs on SGH films and glass slides after 1, 3, 5, and 7 days of culture. After each incubation period, 50 μL of MTT solution (Amresco, USA) was added to each well and incubated for 4 h at 37 °C to allow cell response to occur. This was followed by addition of 150 μL of dimethyl sulfoxide (DMSO, sigma, USA) to dissolve the purple formazan crystals reduced by the living cells. The optical density of the resulting solution was measured using an Ultra Microplate Reader (ELX808; Bio-tek, USA) at 490 nm. Proliferation was re-examined with a non-radioactive fluorometric assay using the DNA-intercalating fluorochrome DAPI (sigma, USA) as previously reported.[59] Briefly, after incubation on SGH films or glass slides for 1, 3, or 5 days, the cells were washed with PBS, and fixed with 4% paraformaldehyde for 30 min. Then DAPI (2 μg/mL) was added to each substrate for 10 min and then visualized under a fluorescence microscope (DMI6000B; Leica, Germany). Five random fields were chosen and the number of DNA-intercalating fluorochrome DAPI was counted.

Cytotoxicity of Seeded rBMSCs: The rBMSCs were incubated on SGH films and glass slides for 24 h, and the potential cytotoxicity was evaluated using the Live/Dead Staining Kit (ScienCell, USA) according to the manufacturer's instructions. Live cells were stained with the polyanionic dye calcein (which fluoresces green), while dead cells with damaged membranes which allowed EthDIII to enter and bind to nucleic acids fluoresced red under the fluorescence microscope (DMI6000B; Leica, Germany).

As a quantitative measure of cytotoxicity, the oxidant-sensitive dye 2′,7′-dichlorofluorescin diacetate (DCFH-DA) was used for reactive oxygen species (ROS) detection (Beyotime Institute of Biotechnology, China). ROS in the cells oxidized DFCH, yielding 2′,7′-dichlorofluorescein (DCF). The rBMSCs were incubated on SGH films and glass slides for 24 h. Then, the culture medium for all cells was replaced with 100 μL of new serum-free medium containing 1 μM DCFH-DA. After incubating at 37 °C for 20 min, the cells were washed three times with serum-free medium to remove unreacted probe molecules, and then the fluorescence intensity was monitored with a fluorescence microscope (DMI6000B; Leica, Germany). Data were taken as the average fluorescence for groups of 20–30 cells.[60] The ROS level was expressed as the ratio of $(F_{test} - F_{blank})/(F_{control} - F_{blank})$, where F_{test} is the fluorescence intensity of the cells incubated on the SGH film or the glass slide, $F_{control}$ is the fluorescence intensity of the cells on the culture dish and F_{blank} is the fluorescence intensity of the substrates without cells.[24]

Implant Procedures: SGH films were cut to a diameter of 6 mm for in vivo implantation. After being incubated in culture medium for 24 h before implantation, the SGH films were implanted into 32 subcutaneous dorsum sites of eight male Fischer rats (body weight 270–300 g). Animals were sacrificed at 2, 4, 8, and 12 weeks following implantation, then implant specimens and major organs were retrieved and fixed in 10% neutralized formalin. The specimens were embedded in paraffin, vertically sectioned (5 μm in thickness) and stained with hematoxylin and eosin (HE) and Trichrome-masson staining for histological evaluation. Images were taken using an Olympus light microscope (BX51; Olympus, Japan).

Alkaline Phosphatase (ALP) Activity Assay: The rBMSCs were seeded onto SGH films and glass slides under culture conditions in either growth medium or osteogenic medium (growth medium with 50 μg/mL L-ascorbic acid, 10 mM glycerophosphate and 100 nM dexamethasone). At 1, 4, and 7 days after cell seeding, ALP activity was evaluated as previously described.[61] Simply put, the cells were detached from discs using trypsin/EDTA, and resuspended in lysis buffer with 0.2% NP-40. Each sample was respectively mixed with 1 mg/mL p-nitrophenyl phosphate (pNPP, Sigma, USA) in 1 M diethanolamine buffer as the substrate and incubated at 37 °C for 15 min. The reaction was stopped by the addition of 3 N NaOH. ALP activity was quantified by absorbance at 405 nm (ELX808; Bio-tek, USA). Total protein content was determined with the Bradford method in aliquots of the same samples with the Bio-Rad protein assay kit (Bio-Rad, USA), read at 630 nm and calculated according to a series of BSA (Sigma, USA) standards. ALP activity was calculated as absorbance at 405 nm (OD value) per milligram of total cellular proteins. All experiments were done in triplicate.

Immunofluorescence Analysis for Osteocalcin (OCN) Protein: The rBMSCs were seeded onto SGH films and glass slides in either growth or osteogenic medium for 1, 4, and 7 days. The cells on both substrates were fixed by 4% paraformaldehyde for 30 min. The anti-OCN primary antibody (Abcam, USA) was added onto the samples at 37 °C for 1 h. After rinsing, fluorescein isothiocyanate (FITC) goat anti-mouse second antibody (Abcam, USA) was added onto each chip and incubated at room temperature for 30 min. The chips were inverted onto glass slides mounted with Vectashield with DAPI (H1200; Vector Lab, USA) and visualized under a fluorescence microscope (DMI6000B; Leica, Germany).

To study the osteoinductivity of the SGH films in the living body, 8 films were implanted into the same positions of another two Fischer rats. Before implantation, a density of 2×10^7 cells/mL rBMSCs were seeded onto the upper sides of the films and incubated for 4 h. Four weeks later, the animals were sacrificed and the implant specimens were retrieved. After freezing in optimal cutting temperature (OTC) compound (Sakura, USA), 8 μm frozen sections were cut in the vertical direction. Sections were fixed with 4% paraformaldehyde for 30 min. After permeabilizing and blocking, anti-OCN antibody (Abcam, USA) was incubated at 37 °C for 1 h. Then red-fluorescent Alexa Fluor 594 goat anti–mouse second antibody (Abcam, USA) was added onto the sections

at room temperature for 30 min. The samples were then mounted using Vectashield with DAPI (H1200; Vector Lab, USA) and observed under a fluorescence microscope (DMI6000B; Leica, Germany).

Alizarin Red S Staining for Calcium-Containing Nodules: The rBMSCs were seeded onto SGH films and glass slides in osteogenic medium for 14 and 28 days. To determine the level of mineralization, calcium-containing nodules were stained by culturing the cells with 10 mg/L Alizarin Red S (Sigma, USA) for 7 days before observation under a fluorescence microscope (DMI6000B; Leica, Germany).

Statistical Analyses: All measurements are presented as mean±standard deviation. Statistical analyses for the assays of rBMSCs seeded onto two substrates were performed by independent sample t-tests assuming equal variance using SPSS (Chicago, IL, USA) 11.0 software. A value of $p < 0.01$ was considered statistically significant.

Supporting Information

Supporting Information is available from the Wiley Online Library or from the author.

Acknowledgements

J.L. and Y.-S.H. contributed equally to this work. This work was supported by the Australian Research Council, the Shanghai Education Committee of China (09JC1411700, 12JC1407301), Shanghai Natural Science Foundation (12ZR1447200), the National Basic Research Program of China (2007CB209705), the Natural Science Foundation of China (21006063) and a China Scholarship Council Fellowship. This work made use of the facilities at the Monash Centre for Electron Microscopy.

Received: December 7, 2012
Revised: January 8, 2013
Published online: February 18, 2013

[1] Y. Zhang, T. R. Nayak, H. Hong, W. Cai, *Nanoscale* **2012**, *4*, 3833.
[2] L. Feng, L. Wu, X. Qu, *Adv. Mater.* **2013**, *25*, 168.
[3] H. Shen, L. Zhang, M. Liu, Z. Zhang, *Theranostics* **2012**, *2*, 283.
[4] K. Yang, L. Feng, X. Shi, Z. Liu, *Chem. Soc. Rev.* **2013**, *42*, 530.
[5] W. Yang, K. R. Ratinac, S. P. Ringer, P. Thordarson, J. J. Gooding, F. Braet, *Angew. Chem. Int. Ed.* **2010**, *49*, 2114.
[6] L. Wang, K. Y. Pu, J. Li, X. Qi, H. Li, H. Zhang, C. Fan, B. Liu, *Adv. Mater.* **2011**, *23*, 4386.
[7] Y. Liu, D. Yu, C. Zeng, Z. Miao, L. Dai, *Langmuir* **2010**, *26*, 6158.
[8] S. He, B. Song, D. Li, C. Zhu, W. Qi, Y. Wen, L. Wang, S. Song, H. Fang, C. Fan, *Adv. Funct. Mater.* **2010**, *20*, 453.
[9] K. Yang, L. Hu, X. Ma, S. Ye, L. Cheng, X. Shi, C. Li, Y. Li, Z. Liu, *Adv. Mater.* **2012**, *24*, 1868.
[10] C. Wang, J. Li, C. Amatore, Y. Chen, H. Jiang, X. M. Wang, *Angew. Chem. Int. Ed.* **2011**, *50*, 11644.
[11] Z. Liu, J. T. Robinson, X. Sun, H. Dai, *J. Am. Chem. Soc.* **2008**, *130*, 10876.
[12] K. Yang, S. Zhang, G. Zhang, X. Sun, S. T. Lee, Z. Liu, *Nano Lett.* **2010**, *10*, 3318.
[13] Z. M. Markovic, L. M. Harhaji-Trajkovic, B. M. Todorovic-Markovic, D. P. Kepic, K. M. Arsikin, S. P. Jovanovic, A. C. Pantovic, M. D. Dramicanin, V. S. Trajkovic, *Biomaterials* **2011**, *32*, 1121.
[14] W. Hu, C. Peng, W. Luo, M. Lv, X. Li, D. Li, Q. Huang, C. Fan, *ACS Nano* **2010**, *4*, 4317.
[15] W. Hu, C. Peng, M. Lv, X. Li, Y. Zhang, N. Chen, C. Fan, Q. Huang, *ACS Nano* **2011**, *5*, 3693.
[16] W. C. Lee, C. H. Lim, H. Shi, L. A. Tang, Y. Wang, C. T. Lim, K. P. Loh, *ACS Nano* **2011**, *5*, 7334.
[17] S. R. Ryoo, Y. K. Kim, M. H. Kim, D. H. Min, *ACS Nano* **2010**, *4*, 6587.
[18] K. S. Novoselov, A. K. Geim, S. V. Morozov, D. Jiang, Y. Zhang, S. V. Dubonos, I. V. Grigorieva, A. A. Firsov, *Science* **2004**, *306*, 666.
[19] C. N. Rao, A. K. Sood, K. S. Subrahmanyam, A. Govindaraj, *Angew. Chem. Int. Ed.* **2009**, *48*, 7752.
[20] A. A. Balandin, S. Ghosh, W. Bao, I. Calizo, D. Teweldebrhan, F. Miao, C. N. Lau, *Nano Lett.* **2008**, *8*, 902.
[21] S. K. Singh, M. K. Singh, P. P. Kulkarni, V. K. Sonkar, J. J. Gracio, D. Dash, *ACS Nano* **2012**, *6*, 2731.
[22] K. Yang, J. Wan, S. Zhang, Y. Zhang, S. T. Lee, Z. Liu, *ACS Nano* **2011**, *5*, 516.
[23] D. Li, M. B. Muller, S. Gilje, R. B. Kaner, G. G. Wallace, *Nat. Nanotechnol.* **2008**, *3*, 101.
[24] Y. Chang, S. T. Yang, J. H. Liu, E. Dong, Y. Wang, A. Cao, Y. Liu, H. Wang, *Toxicol. Lett.* **2011**, *200*, 201.
[25] O. N. Ruiz, K. A. Fernando, B. Wang, N. A. Brown, P. G. Luo, N. D. McNamara, M. Vangsness, Y. P. Sun, C. E. Bunker, *ACS Nano* **2011**, *5*, 8100.
[26] H. Fan, L. Wang, K. Zhao, N. Li, Z. Shi, Z. Ge, Z. Jin, *Biomacromolecules* **2010**, *11*, 2345.
[27] N. Li, X. Zhang, Q. Song, R. Su, Q. Zhang, T. Kong, L. Liu, G. Jin, M. Tang, G. Cheng, *Biomaterials* **2011**, *32*, 9374.
[28] X. Yan, J. Chen, J. Yang, Q. Xue, P. Miele, *ACS Appl. Mater. Interfaces* **2010**, *2*, 2521.
[29] G. Y. Chen, D. W. Pang, S. M. Hwang, H. Y. Tuan, Y. C. Hu, *Biomaterials* **2012**, *33*, 418.
[30] Q. H. Wang, Z. Jin, K. K. Kim, A. J. Hilmer, G. L. Paulus, C. J. Shih, M. H. Ham, J. D. Sanchez-Yamagishi, K. Watanabe, T. Taniguchi, J. Kong, P. Jarillo-Herrero, M. S. Strano, *Nat. Chem.* **2012**, *4*, 724.
[31] X. Yang, J. Zhu, L. Qiu, D. Li, *Adv. Mater.* **2011**, *23*, 2833.
[32] X. Yang, L. Qiu, C. Cheng, Y. Wu, Z. F. Ma, D. Li, *Angew. Chem. Int. Ed.* **2011**, *50*, 7325.
[33] T. R. Nayak, H. Andersen, V. S. Makam, C. Khaw, S. Bae, X. Xu, P. L. Ee, J. H. Ahn, B. H. Hong, G. Pastorin, B. Ozyilmaz, *ACS Nano* **2011**, *5*, 4670.
[34] C. Cheng, J. Uhe, X. Yang, Y. Wu, D. Li, *Prog. Nat. Sci.* **2012**, *22*, 670.
[35] J. Zhu, C. Cheng, X. Yang, Y. Wang, L. Qiu, D. Li, *Chem. -Eur. J.* DOI: 10.1002/chem.201203219.
[36] L. Qiu, X. Zhang, W. Yang, Y. Wang, G. P. Simon, D. Li, *Chem. Commun.* **2011**, *47*, 5810.
[37] J. He, W. Zhou, X. Zhou, X. Zhong, X. Zhang, P. Wan, B. Zhu, W. Chen, *J. Mater. Sci.: Mater. Med.* **2008**, *19*, 3465.
[38] M. Kalbacova, A. Broz, J. Kong, M. Kalbac, *Carbon* **2010**, *48*, 4323.
[39] H. N. Lim, N. M. Huang, S. S. Lim, I. Harrison, C. H. Chia, *Int. J. Nanomed.* **2011**, *6*, 1817.
[40] K. H. Liao, Y. S. Lin, C. W. Macosko, C. L. Haynes, *ACS Appl. Mater. Interfaces* **2011**, *3*, 2607.
[41] J. A. Hunt, D. F. Williams, *Biomaterials* **1995**, *16*, 167.
[42] P. Kallio, J. E. Michelsson, M. Lalla, T. Holm, *J. Bone Joint Surg., Br. Vol.* **1990**, *72*, 615.
[43] D. Zou, L. Guo, J. Lu, X. Zhang, J. Wei, C. Liu, Z. Zhang, X. Jiang, *Tissue Eng., Part A* **2012**, *18*, 1464.
[44] A. Abarrategi, M. C. Gutierrez, C. Moreno-Vicente, M. J. Hortiguela, V. Ramos, J. L. Lopez-Lacomba, M. L. Ferrer, F. del Monte, *Biomaterials* **2008**, *29*, 94.
[45] J. S. Temenoff, A. G. Mikos, *Biomaterials: The Intersection of Biology and Materials Science*, Pearson/Prentice Hall, Upper Saddle River, NJ **2008**, Ch.5.
[46] L. Xia, Z. Zhang, L. Chen, W. Zhang, D. Zeng, X. Zhang, J. Chang, X. Jiang, *Eur. Cell. Mater.* **2011**, *22*, 68.

[47] M. F. Pittenger, *Science* **1999**, *284*, 143.
[48] R. Okazaki, *Endocrinology* **2002**, *143*, 2349.
[49] W. R. Duarte, T. Shibata, K. Takenaga, E. Takahashi, K. Kubota, K. Ohya, I. Ishikawa, M. Yamauchi, S. Kasugai, *J. Bone Miner. Res.* **2003**, *18*, 493.
[50] S. Catros, N. Zwetyenga, R. Bareille, B. Brouillaud, M. Renard, J. Amedee, J. C. Fricain, *J. Orthop. Res.* **2009**, *27*, 155.
[51] R. McBeath, D. M. Pirone, C. M. Nelson, K. Bhadriraju, C. S. Chen, *Dev. Cell* **2004**, *6*, 483.
[52] S. Oh, K. S. Brammer, Y. S. Li, D. Teng, A. J. Engler, S. Chien, S. Jin, *Proc. Natl. Acad. Sci. USA* **2009**, *106*, 2130.
[53] M. J. Dalby, N. Gadegaard, R. Tare, A. Andar, M. O. Riehle, P. Herzyk, C. D. Wilkinson, R. O. Oreffo, *Nat. Mater.* **2007**, *6*, 997.
[54] A. J. Engler, S. Sen, H. L. Sweeney, D. E. Discher, *Cell* **2006**, *126*, 677.
[55] J. McMillan, R. C. Kinney, D. M. Ranly, S. Fatehi-Sedeh, Z. Schwartz, B. D. Boyan, *Bone* **2007**, *40*, 111.
[56] H. Chen, M. B. Müller, K. J. Gilmore, G. G. Wallace, D. Li, *Adv. Mater.* **2008**, *20*, 3557.
[57] C. Maniatopoulos, J. Sodek, A. H. Melcher, *Cell Tissue Res.* **1988**, *254*, 317.
[58] H. Sun, C. Wu, K. Dai, J. Chang, T. Tang, *Biomaterials* **2006**, *27*, 5651.
[59] M. Brzoska, H. Geiger, S. Gauer, P. Baer, *Biochem. Biophys. Res. Commun.* **2005**, *330*, 142.
[60] N. S. Chandel, E. Maltepe, E. Goldwasser, C. E. Mathieu, M. C. Simon, P. T. Schumacker, *Proc. Natl. Acad. Sci. USA* **1998**, *95*, 11715.
[61] Q. Liu, L. Cen, S. Yin, L. Chen, G. Liu, J. Chang, L. Cui, *Biomaterials* **2008**, *29*, 4792.